Modelling of Viscoelasticity in Pressure-Volume Curve of an Intact Gallbladder

Wenguang Li

School of Engineering

University of Glasgow, Glasgow, G12 8QQ, UK

E-mail:wenguang.li@glasgow.ac.uk

Date: 26/05/2020

Abstract

Like other organs such as artery, bladder and left ventricle, human intact gallbladders (GB) possess viscoelasticity/hysteresis in pressure-volume curves during in vitro or in vivo dynamic experiments made by using saline infusion and withdrawal cycle to simulate GB physiological emptying-filling cycle in normal and diseased conditions. However, such a viscoelastic property of GBs hasn't been modelled and analysed so far. A nonlinear discrete viscous model and a passive elastic model were proposed to identify the elastic, active and viscous pressure responses in the experimental pressure-volume data of an intact GB under passive and active conditions found in the literature in the paper. It turns out that the elastic, viscous and active pressure responses can be separated in less than 2% error from the pressure-volume curves. The peak active state in the GB occurs at 30% dimensionless volume. The GB stimulated with cholecystokinin (CCK) or treated with indomethacin is subject to almost constant stiffness at low dimensionless volume ($\leq 70\%$) but quick increasing stiffness at high dimensionless volume ($>70\%$) and a larger work-to-energy ratio (0.57-0.61) compared with the normal GB in passive state. The models are sensitive to the change in biomechanical property of the GBs stimulated or treated with hormonal or pharmacological agents, showing a potential in clinical application. These results may contribute fresh content to biomechanics of GBs and be helpful to GB disease diagnosis.

Keywords: gallbladder; viscoelasticity; hysteresis loop; pressure-volume curve; passive state; active state

Nomenclature

a_1, a_2, a_3	model constants of viscosity in passive state
b_1, b_2, b_3	model constants of viscosity in active state
c_0, c_1, c_2, c_3	model constants of GB pressure-volume curve
E	elastic energy stored in GB wall during its elastic deformation, N.m
F	objective function
i	an experimental point
k	stiffness of GB pressure-volume curve
m_1	model constant of viscosity in passive state
m_2	model constant of viscosity in active state
n_1, n_2	model constants of GB pressure-volume curve
N	number of experimental points
p	pressure, mmHg or cm H_2O
t	time, min

t_1, t_2, t_3 time moments at the start of infusion, end of infusion and end of withdrawal, min

v dimensionless GB volume

V GB bile volume, ml

W work done on viscous response in infusion-withdrawal cycle, N.m

Greek letters

γ work-to-energy ratio, $\gamma = W/E$

ε error in pressure in passive and active states, %

η viscosity of dashpot

Subscripts

1 passive state

2 active state

e elastic

exp experimental

f infusion

max maximum value

p pressure

v viscous

w withdrawal

Abbreviation

3D three-dimensional

ABP acalculous biliary pain

CCK cholecystokinin

EF ejection fraction

GB gallbladder

1 Introduction

Acalculous biliary pain (ABP) is a common clinical problem [1]. Laparoscopic cholecystectomy (LC) has been conducted on patients with ABP with cholecystokinin (CCK) infusion [3-10]. Unfortunately, the patients with persistent symptom still can be as many as 20% after LC [2]. More recently, clinical trials show that the majority of ABP patients can have resolution of painful symptom, but the gallbladder (GB) bile ejection fraction (EF) doesn't predict outcome and the patients with normal GB EF are subject to a less benefit from LC.

ABP can involve biomechanical factors. GB smooth muscle is subject to an impaired contractile capacity in response to CCK [11], and the smooth muscle to fibrosis layer thickness ratio might be associated with abnormal EF [12]. These two factors can alter the bile pressure in a GB and the stress level in the GB wall. Total (active plus passive) peak stress was estimated at the start of GB emptying phase in CCK-ultrasound scan examinations based on an ellipsoid model in [13,14]. It turned out that the peak stress can correlate to the ABP symptom well. These investigations are completely based on GB static biomechanical behaviour.

However, human GB works under dynamic condition with emptying-filling cycle. Thus a few series of in vitro experiments on GB dynamic behaviour have been carried out by making use of saline infusion and withdrawal in passive and active states [15-18] even though saline infusion-withdrawal cycle may differ from the GB physiological emptying-filling cycle. A typical experimental set-up sketch, pressure-time and pressure-volume curves are illustrated in Fig.1. Clearly, the pressure path in the infusion is different from that in the withdrawal, forming a hysteresis loop. It is not surprised that intact GB exhibits viscoelasticity like aorta [19], artery [20-23], bladder [24], left ventricle [25,26] and so on. However, this hysteresis loop in the pressure-volume curve of an intact GB has never been studied analytically in terms of viscoelastic context in the literature so far.

Existing viscoelastic models for soft tissues can be classified into four types: (1) discrete model in time domain, (2) discrete model in frequency domain, (3) quasi-linear model or continuous model in time domain and (4) viscous potential function model in time domain. In the discrete model in time domain, a soft tissue is represented with a spring and a dashpot in series (Maxwell model) or in parallel (Voigt model) or their combinations [27] and time is independent variable. The model can be with linear spring and linear dashpot [28] or exponential spring and linear dashpot [29] or linear spring and nonlinear dashpot [30] or a spring with isotropic exponential strain energy function and linear dashpot [31] or a spring with neo-Hookean strain energy function and nonlinear dashpot with power function [32].

In the discrete model in frequency domain, a soft tissue is still represented with a spring and a dashpot in series or in parallel or their combinations but the governing equation of the model is transformed to the frequency domain with Laplace transform, and frequency is independent variable. In this sort of model, the complex Young modulus can be easily calculated. Once the solution is obtained

in the frequency domain, it can be mapped back to the time domain by employing inverse Laplace transform [33-35].

In the quasi-linear model or continuous model in time domain or Fung model, the stress in a soft tissue is equal to the product of an elastic stress and a reduced relaxation function [36-49]. The total stress is calculated from a convolution integral between the reduced relaxation function and the rate of elastic stress. The reduced relaxation function is determined by means of relaxation test data. The elastic stress function is decided by using total stress elongation test data at various strain rates.

In the viscous potential function model in time domain, the elastic stress is expressed with a strain energy function and the viscous stress is in terms of viscous potential function which is as a function a few invariants related to viscoelasticity and strain rate, especially for short-term visco-elasticity [50-57], the property constants are determined by using stress-strain curves at various strain rates.

It is suspected that the hysteresis effect or dynamic behavior of an intact GB may have a close link to ABP. To achieve that final goal, as a first step, a nonlinear viscous model and a passive elastic model were proposed in terms of the discrete Voigt viscoelastic model in time domain to identify the elastic and viscous responses in the experimental pressure-volume data of an intact GB under passive and active conditions found in the literature in this paper. The ratio of the work done on the viscous response to the elastic energy and the stiffness of the elastic pressure-volume curve were defined and extracted. The established models are sensitive to variations in biomechanical property when GBs are stimulated with CCK and treated with indomethacin. The viscoelastic models presented here may be meaningful to better understanding of GB biomechanical behavior and benefits ABP or other diseases diagnosis in the future.

2 Experiment and Method

2.1 Experiment

In vitro experimental measurements on pressure in the guinea pig GB were made in [16] under passive and active conditions. During experiments, a guinea pig was anesthetized with urethane and laparotomy operated, a catheter sutured into the fundus of the GB was connected to an infusion-withdrawal pump and a pressure sensor as shown in Fig. 1a. CCK was infused at 0.6 Ivy dog units/kg/min by using a catheter inserted in the inferior vena cava over 20min. The GB pressure-volume curve was recorded continuously with a computer in infusion (lasting 2min) and withdrawal (2min). The recorded GB pressure-time history curves and pressure-volume curves are illustrated in Fig.1b and 1c under passive and CCK stimulated conditions for the same GB. The GB volume is in terms of percentage of the maximum GB volume. In the two conditions, the GB pressure-volume curves in infusion and withdrawal processes are in difference paths, exhibiting a hysteresis effect. In the paper, this effect will be modelled by using nonlinear discrete viscoelastic models based on these experimental data.

2.2 Biomechanical Model

The GB is composed of three layers: a mucosa, muscularis externa and adventitia (serosa), see Fig.2. The very tall, simple columnar epithelium of the mucosa forms a number of folds to absorb water in the bile effectively. The mucosa is full of vascular vessels but without lymphatics. The muscle layer includes the longitudinal smooth muscle fibres along the longitudinal direction near the lamina propria and circular smooth muscle fibres near the adventitia layer. These smooth muscle fibres contribute to contraction as the GB is under stimulation of CCK. The adventitia layer consists of collagen fibres such as I, III and IV types and fibronectin [58] as well as elastin, which are responsible for GB passive expansion and shrinkage.

Borne that GB layer structure in mind, from the biomechanical point of view, the GB wall is regarded as three nonlinear springs, one contractile element, and one nonlinear dashpot in parallel phenomenologically and biomechanically, as shown in Fig.3. In passive state, the elastic pressure response p_e is related to the apparent stiffness of elastin and matrix, collagen fibre and smooth muscle, that the viscous pressure response p_v exists is owing to the dashpot, the cross-bridges in the muscle are not in engagement, so that the active response is zero, p_a=0 [59]. The collagen fibres engage at high GB volume only. In active stage, except the three passive springs and one dashpot, the active pressure response p_a comes into play as the cross-bridges are in engagement. Due to effect of CCK, the model parameters for a GB wall in passive state can differ from those in active state resulted by contraction.

The pressure-volume curves shown in Fig.1c are decomposed into three components, namely, passive, active and viscoelastic components to match respective responses of elastic, contractile and viscoelastic elements in parallel in the GB wall tissue. In the passive state experiment, the pressure p_{1f} in infusion process and p_{1w} in withdrawal process are divided into the pressures for elastic and viscous responses, and expressed as follows

$$\begin{cases} p_{1f} = p_{1fe}(V) + p_{1fv}\left(dp_{1f}/dt\right) & \text{infusion} \\ p_{1w} = p_{1we}(V) + p_{1wv}(dp_{1w}/dt) & \text{withdrawal} \end{cases} \tag{1}$$

where $p_{1fe}(V)$ and $p_{1we}(V)$ are the pressures for the elastic responses in infusion and withdrawal processes, $p_{1fv}\left(dp_{1f}/dt\right)$ and $p_{1wv}(dp_{1w}/dt)$ are the pressures for the viscous responses in infusion and withdrawal processes.

Firstly, $p_{1fe}(V)$ and $p_{1fv}\left(dp_{1f}/dt\right)$, $p_{1we}(V)$ and $p_{1wv}(dp_{1w}/dt)$ are determined based on the pressure-volume data in a passive state experiment. $p_{1fv}\left(dp_{1f}/dt\right)$ is supposed to be the product of nonlinear viscosity $\eta_1\left(dp_{1f}/dt\,, a_1, a_2, a_3, m_1\right)$ and dp_{1f}/dt, while $p_{1wv}(dp_{1w}/dt)$ is the product of nonlinear viscosity $\eta_1(dp_{1w}/dt\,, a_1, a_2, a_3, m_1)$ and dp_{1w}/dt. Note that dp_{1f}/dt and dp_{1w}/dt are known in the experiment, and the viscosity function η_1 and its constants a_1, a_2, a_3, m_1 can be determined with the experimental pressure-volume curves. $p_{1fe}(V)$ and $p_{1we}(V)$ are calculated by the following expressions

$$\begin{cases} p_{1fe}(V_i) = p_{1f,exp}(V_i) - \eta_1\left(dp_{1f}/dt\,, a_1, a_2, a_3, m_1\right) dp_{1f}/dt & \text{infusion} \\ p_{1we}(V_i) = p_{1w,exp}(V_i) - \eta_1(dp_{1w}/dt\,, a_1, a_2, a_3, m_1)\, dp_{1w}/dt & \text{withdrawal} \end{cases} \tag{2}$$

where $p_{1fe}(V_i)$ and $p_{1we}(V_i)$ are elastic response in infusion and withdrawal processes at a GB specific volume V_i. $p_{1fe}(V_i)$ and $p_{1we}(V_i)$ are independent of loading paths. Hence the proper constants a_1, a_2, a_3, m_1 should make the following objective function minimum

$$F_1 = \sum_{i=1}^{N}\left[p_{1fe}(V_i) - p_{1we}(V_i)\right]^2 \tag{3}$$

where N is the number of experimental data points.

Secondly, for the same intact GB in active state, the pressure decomposition for elastic and viscous responses is expressed as follows in infusion and withdrawal processes

$$\begin{cases} p_{2f} = p_{2fe}(V) + p_{2fv}\left(dp_{2f}/dt\right) & \text{infusion} \\ p_{2w} = p_{2we}(V) + p_{2wv}(dp_{2w}/dt) & \text{withdrawal} \end{cases} \tag{4}$$

where $p_{2fv}\left(dp_{2f}/dt\right)$ is a function of both dp_{2f}/dt and nonlinear viscosity $\eta_2\left(dp_{2f}/dt\,, b_1, b_2, b_3, m_2\right)$, this is true for $p_{2wv}(dp_{2w}/dt)$. They are estimated by the following expressions

$$\begin{cases} p_{2fe}(V_i) = p_{2f,exp}(V_i) - \eta_2\left(dp_{2f}/dt\,, b_1, b_2, b_3, m_2\right) dp_{2f}/dt & \text{infusion} \\ p_{2we}(V_i) = p_{2w,exp}(V_i) - \eta_2(dp_{2w}/dt\,, b_1, b_2, b_3, m_2)\, dp_{2w}/dt & \text{withdrawal} \end{cases} \tag{5}$$

where $p_{2fe}(V_i)$ and $p_{2we}(V_i)$ are independent of loading path. Therefore, the proper constants b_1, b_2, b_3, m_2 should make the following objective function minimum as well

$$F_2 = \sum_{i=1}^{N}\left[p_{2fe}(V_i) - p_{2we}(V_i)\right]^2 \tag{6}$$

Thirdly, the pressure for active response $p_a(V_i)$ at each experimental data point is calculated by

$$\begin{cases} p_a(V_i) = p_{2e}(V_i) - p_{1e}(V_i) \\ p_{1e}(V_i) = 0.5\left[p_{1fe}(V_i) + p_{1we}(V_i)\right] \\ p_{2e}(V_i) = 0.5\left[p_{2fe}(V_i) + p_{2we}(V_i)\right] \end{cases} \tag{7}$$

then, the mathematical models of pressure passive and active components can be established based on the data points of $p_{1e}(V_i)$ and $p_a(V_i)$. In this way, the dynamic behaviour of an intact GB can be resolved.

Finally, the extracted $p_{1e}(V_i)$, $p_a(V_i)$, $p_{1fv}(V_i) - p_{1wv}(V_i)$ and $p_{2fv}(V_i) - p_{2wv}(V_i)$ curves are analysed in terms of existing clinical observations to provide some insight into GB dynamic behaviour.

The viscous biomechanical model is essential for solving Eqs. (2) and (5). Thus, the following viscous biomechanical model is proposed for the nonlinear dashpot in passive state

$$\begin{cases} \eta_1\left(\frac{dp_{1f}}{dt}, a_1, a_2, a_3, m_1\right)\frac{dp_{1f}}{dt} = \left(a_1 + a_2\left|\frac{dp_{1f}}{dt}\right|^{m_1} + a_3\left|\frac{dp_{1f}}{dt}\right|^{2m_1}\right)\frac{dp_{1f}}{dt} \\ \eta_1\left(\frac{dp_{1w}}{dt}, a_1, a_2, a_3, m_1\right)\frac{dp_{1w}}{dt} = \left(a_1 + a_2\left|\frac{dp_{1w}}{dt}\right|^{m_1} + a_3\left|\frac{dp_{1w}}{dt}\right|^{2m_1}\right)\frac{dp_{1w}}{dt} \end{cases} \tag{8}$$

Likewise, in active state, the viscous biomechanical model reads

$$\begin{cases}\eta_2\left(\frac{dp_{2f}}{dt}, b_1, b_2, b_3, m_2\right)\frac{dp_{2f}}{dt} = \left(b_1 + b_2\left|\frac{dp_{2f}}{dt}\right|^{m_2} + b_3\left|\frac{dp_{2f}}{dt}\right|^{2m_2}\right)\frac{dp_{2f}}{dt} \\ \eta_2\left(\frac{dp_{2w}}{dt}, b_1, b_2, b_3, m_2\right)\frac{dp_{2w}}{dt} = \left(b_1 + b_2\left|\frac{dp_{2w}}{dt}\right|^{m_2} + b_3\left|\frac{dp_{2w}}{dt}\right|^{2m_2}\right)\frac{dp_{2w}}{dt}\end{cases} \quad (9)$$

where the property constants a_2 and b_2 are negative, but the rest constants are positive in Eqs.(8) and (9).

At three specific time moments, namely the start of infusion, t_1, the end of infusion, t_2, and the end of withdrawal, t_3, the slopes dp_{1f}/dt, dp_{1w}/dt, dp_{2f}/dt and dp_{2w}/dt should be zero, i.e.

$$\frac{dp_{1f}}{dt} = \frac{dp_{1w}}{dt} = \frac{dp_{2f}}{dt} = \frac{dp_{2w}}{dt} = 0 \text{ at } t = t_1, t_2, t_3 \quad (10)$$

where t_1=0, t_2=2, and t_3=4min based on Fig. 1b.

The scattered data points in Fig. 1b are best fitted by using a 4th or 3rd-order polynomial, and then its derivative with respect to time is derived to obtain experimental slopes dp_{1f}/dt, dp_{1w}/dt, dp_{2f}/dt and dp_{2w}/dt. In passive state, their expressions are written as

$$\begin{cases}\frac{dp_{1f}}{dt} = -4 \times 3.3052t^3 + 3 \times 14.155t^2 - 2 \times 18.983t + 15.722 \\ \frac{dp_{1w}}{dt} = -4 \times 3.0114t^3 - 3 \times 41.538t^2 + 2 \times 215.06t - 499.03\end{cases} \quad (11)$$

Whilst in active state, the expressions are deduced as follows

$$\begin{cases}\frac{dp_{2f}}{dt} = -4 \times 6.7026t^3 + 3 \times 32.28t^2 + 2 \times 54.1770t + 44.842 \\ \frac{dp_{2w}}{dt} = -3 \times 4.4689t^2 + 2 \times 47.664t - 127.54\end{cases} \quad (12)$$

The condition expressed with Eq. (10) should be imposed in Eqs. (11) and (12), even though these slopes may not be exactly zero at t_1=0, t_2=2, and t_3=4min.

After the passive elastic pressure-volume scattered points are extracted, they should be regressed with a mathematical model. Based on existing experimental GB pressure-volume data in passive and active states, the following mathematical model is proposed in terms of dimensionless GB volume

$$p_e = p_{e,exp}(0) + c_0 v + c_1 v^{n_1} + c_2 e^{c_3 v^{n_2}} \quad (13)$$

where v is dimensionless GB volume, $v = V/V_{max}$, V_{max} is the largest GB volume achievable in an experiment, V is a GB volume less than V_{max}, $p_{e,exp}(0)$ is the GB pressure at v=0 in the experiment, c_0, c_1, c_2, c_3, n_1 and n_2 are model constants and will be determined by employing a set of experimental pressure-volume data. A validation of Eq. (13) is present in Appendix against eight sets of GB experimental pressure-volume data in passive and active states.

3 Results

The biomechanical model and experimental data of a guinea-pig GB in [16] were coded in MATLAB® R2018b. Firstly, the pressure-volume curves for the elastic and viscous responses in passive and active states are split by employing the *lsqnonlin* function based on the trust-region-reflective optimization algorithm, then the elastic pressure-volume curves in both the states are best fitted by using Eq. (13). The determined model constants and errors in the two procedures are listed in Table 1. The

errors in passive and active states, ε_1 and ε_2 are defined as

$$\begin{cases} \varepsilon_1 = \dfrac{\sqrt{F_1}}{0.5\sum_{i=1}^{N}[p_{1f,exp}(V_i)+p_{1w,exp}(V_i)]} \times 100\% \\ \varepsilon_2 = \dfrac{\sqrt{F_2}}{0.5\sum_{i=1}^{N}[p_{2f,exp}(V_i)+p_{2w,exp}(V_i)]} \times 100\% \end{cases} \tag{14}$$

The split elastic and viscous pressure-volume curves are illustrated in Fig.4 along with the experimental data, and the elastic passive and active pressure-volume curves are shown, too. It is shown that the errors, ε_1 and ε_2 are all less than 2%, suggesting the biomechanical models proposed are feasible and reasonable.

The extracted viscous pressure-volume curves are very similar to those from the experimental data. As a result, the error in the areas enclosed by the curves and the horizontal axis in Fig. 4c is less than 1% between the experiments and the model predictions.

In Fig.4d, the extracted elastic pressures, p_{1e} and p_{2e} can be best fitted by using the model expressed with Eq. (13), giving the errors as small as 0.6% and 1.0%, respectively. The active pressure response can be best fitted by employing a polynomial as done in [60,61] for smooth muscle in active state as the following

$$p_a = -3.3519 \times 10^{-7}v^4 + 9.2538 \times 10^{-5}v^3 - 9.11 \times 10^{-3}v^2 + 3.4058 \times 10^{-1}v + 2.2114 \tag{15}$$

where the correlation coefficient of the equation remains to be 0.84. The peak active state occurs at 30%.

The influence of indomethacin on guinea-pig gallstone formation and motility in control and cholesterol-fed was examined [16]. It was indicated that indomethacin can diminish GB mobility or tone. To clarify this from the biomechanical point of view, the pressures for elastic and viscous response are extracted as well. The experimental pressure-time and pressure-volume curves in infusion and withdrawal are illustrated in Fig.5a and 5b, the slopes of the pressure-time curves are expressed as

$$\begin{cases} \frac{dp_{1f}}{dt} = -6 \times 3.6236t^5 + 5 \times 23.9049t^4 - 4 \times 61.192t^3 + 3 \times 77.8922t^2 - 2 \times 51.5662t + 20.1179 \\ \frac{dp_{1w}}{dt} = 6 \times 0.0644t^5 - 5 \times 1.8649t^4 + 4 \times 21.7908t^3 - 3 \times 130.824t^2 + 2 \times 427.1563t - 725.1213 \end{cases} \tag{16}$$

Based on the method in Section 2 in passive state, the extracted elastic pressure-volume curve is illustrated in Fig.5b, and the pressure-volume curves for viscous response are demonstrated in Fig.5c, the determined model constants are listed in Table 1. In terms of the errors in the table, the method proposed in Section 2 is applicable to the GB treated with indomethacin.

To clarify the difference in biomechanical properties of GBs in CCK stimulated and normal passive states as well as under the condition treated with indomethacin, the ratio of the work done on the viscous response in the hysteresis loop to the elastic energy is proposed, which is defined as

$$\gamma = \frac{W}{E}, W = \oint p_v dV\,,\ E = \int_0^{V_{max}} p_e dV \tag{17}$$

where γ is the work-to-energy ratio, E and W are the elastic energy stored and the work done by loading, p_v is the pressure for viscous response, p_e is the pressure for elastic response.

Additionally, the stiffness of the elastic pressure-volume curve expressed with Eq. (13) is extracted

with the following expression

$$k = \frac{dp_e}{dv} = c_0 + c_1 n_1 v^{n_1 - 1} + c_2 c_3 n_2 v^{n_2 - 1} e^{c_3 v^{n_2}} \quad (18)$$

where k is the stiffness and the powers are $n_1, n_2 > 0$.

The ratio γ and stiffness k are illustrated in Fig.6 in terms of dimensionless GB volume. The biomechanical behaviour of the GB stimulated with CCK or treated with indomethacin is considerably different from the normal GB in passive state. The former is subject to a flatter stiffness at low volume ($v \leq 0.7$) and a sharper stiffness at high volume ($v > 0.7$) and a larger work-to-energy ratio (0.57-0.61) in comparison with the normal GB in passive state. These facts demonstrate that the two chemicals may have altered the biomechanical behaviour of the GB wall. The biomechanical model developed in the paper is sensitive to such a change in the biomechanical property.

4 Discussion

In the paper, a biomechanical method was proposed for identifying elastic and viscous responses to saline infusion and withdrawal in vitro in a guinea pig GB by employing the nonlinear Voigt model in terms of the slope of pressure-time curves under passive and active conditions. An innovative mathematical model was devised for fitting the elastic pressure-volume response of intact GBs. Such an analytical study has been unavailable to intact GBs so far. The method is meaningful to clarifying viscous and elastic properties in the hysteresis loop of diseased or healthy GBs under active and passive conditions. It is potentially applicable to GB disease diagenesis or pathological assessment.

An approach was raised in [62] for separating elastic and viscous responses in the hysteresis loop in monitored arterial stress-radius curves in terms of the slope of radius-time relationships and a 2nd-order viscous model was adopted. The method presented herein was inspired by [62] honestly, but there are different in two aspects, namely (1) a new nonlinear viscous model is specified and (2) a general biomechanical model for elastic pressure-volume curves of GBs is put forward for passive and active GBs.

In the present paper, the slopes dp_{1f}/dt, dp_{1w}/dt etc were used as an independent variable in the viscous model. In Fig.7, the pressure- and volume-time curves of a baboons GB are illustrated in infusion-withdrawal cycle of saline volume. Based on the figure, it is seen that the GB pressure and volume vary in almost identical phase angle and the frequency of infusion-withdrawal cycle is 1/20Hz [15]. The experimental data in [16] were analysed in the paper. The frequency of infusion-withdrawal cycle is 1/240Hz, which is 1/12th of 1/20Hz, hence the GB pressure and volume in [16] will be in the same phase angle during the cycle. In this context, that the slopes dp_{1f}/dt, dp_{1w}/dt etc were considered an independent variable in the viscous model is reasonable and feasible.

In GB infusion-withdrawal cycle experiments, the frequency of the infusion-withdrawal cycle can influence the viscoelastic property of intact GBs. For example, the hysteresis loop size is expanded largely as the frequency is at 0.17Hz and 3.33Hz in passive guinea pig GBs, respectively. However, the

loop size is the narrowest at the frequency of 1.67Hz [18].

The mean time scales of emptying(withdrawal) are 10min and 18min for the human healthy GBs and the GBs with gallstone, while the filling (infusion) time scales are 60min [63]. Based on these time scales, the frequencies of emptying(withdrawal)-filling(infusion) cycle can be as low as 1/4200Hz for the healthy GBs and 1/4680Hz for the GBs with gallstone. Therefore, there is a significant difference in the frequency of infusion-withdrawal cycle in experiment from physiology, but also the emptying is much faster than the filling. Whether there is the viscoelastic property in human intact GBs at such a low frequency of emptying-filling cycle needs a confirmation in the future.

CCK is a peptide hormone to contract GB muscle by attaching to CCK receptors imbedded in the smooth muscle of the GB [64,65]. The change in the stiffness of the passive elastic pressure-volume curve of the GB stimulated with CCK occurs mainly at a large GB volume compared with the normal GB as shown in Fig.6a. This effect seems to suggest CCK may lead to significant alternation in the passive biomechanical property of the smooth muscle at large GB volume.

Indomethacin is a nonsteroidal anti-inflammatory drug (NSAID) blocking the production of prostaglandins which influence smooth muscle contractility but also relieve inflammation. It was shown that indomethacin can reduce or abolish GB smooth muscle spontaneous rhythmical contractions by inhibiting endogenous prostaglandin synthesis [16,66,67]. A few studies suggested indomethacin can improve GB emptying of patients with gallstones [68] or animal models with cholecystitis [54], but has no effect on healthy GBs [69,70]. Based on those observations, it is confirmed that the change in biomechanical property of GB smooth muscle is attributed to indomethacin. In Fig 6a, however, indomethacin apparently reduces the stiffness of the passive pressure-volume curve starkly at low and large GB volumes, implying indomethacin may alter the biomechanical property of the other components such as elastin and collagen fibre. Obviously, the corresponding experimental evidence is on demand.

Note that the GB pressure-volume curve based on in vitro infusion-withdrawal cycle differs from that in physiological state, as sketched in Fig. 8a. The GB pressure-volume curve in the physiological state includes a contraction phase [71], but that pressure-volume curve in infusion-withdrawal cycle experiments hasn't the phase. Additionally, the hysteresis loop sense in the infusion-withdrawal cycle is opposite to that in the filling-emptying cycle. These facts show that the infusion-withdrawal cycle experiment differs from the physiological filling-emptying cycle and is essentially an in vitro or in vivo method for characterizing the viscoelastic biomechanical property of an intact GB only, then has nothing to do with the physiological filling-emptying cycle of GBs. If the viscous effect in the GB wall is considered in the GB filling-emptying cycle, the cycle should be like one in dashed lines shown in Fig.8b. If the effect is strong enough, it will impair the GB motor function.

The paper is preliminary in method and results and faces a few limitations inevitably. Firstly, the two models proposed in the paper are phenomenological at organ level. And the models need to be updated to new versions with information of the microstructure of GB wall in the future. Secondly, a

nonlinear discrete dashpot model was proposed in the paper. The model takes an advantage of less number of model constants than the quasi-linear model or continuous model where the constants in the elastic model and the reduced relaxation function (Prony series) for viscous effect must be determined simultaneously. However, the quasi-linear remodel is more general and likely finds applications in GBs in the future.

Thirdly, based on the present methods proposed here the elastic, active and viscous pressure-volume curves have been separated for the GB. If the GB geometrical parameters were known with volume change, then the corresponding 3D elastic, active and viscous stresses would be estimated by using the simple ellipsoid model of the GB [13,14]. Or the strain energy function for the elastic response proposed in [71] is applied to GB walls, then the empirical viscosity as expressed with Eq. (8) or (9) is involved into the total stress equation by using the methods in [32,49], eventually 3D stress in the GB wall can be calculated in passive state. Once again, the constants in the elastic strain energy function and viscous model must be decided by using experimental data in one go, and the model might suffer from too many model constants. Since the geometrical parameters of the experimental GB were not provided in [16], these stress estimates cannot be workable in the paper. Nevertheless, the viscous potential function model, specially the short-term viscous potential function in emptying phase and long-term viscous potential function in filling phase, is worthy of being attempted with a complete set of experimental data of an intact GB in the future.

5 Conclusion

Nonlinear viscous and elastic models were developed to identify the elastic, viscous and active pressure responses in the pressure-volume curves of a guinea-pig intact GB when the GB was pressurised and depressurised with infusion and withdrawal of an amount volume of saline continuously in passive and active states in the article. The new model for describing GB elastic pressure-volume curves was proposed and validated with the experimental data of rabbit, guinea-pig and human intact GBs. It was demonstrated that the elastic, viscous and active pressure responses can be separated in less than 2% error from the pressure-volume curves of the intact GB as it is in passive and active states, respectively. The peak active state in the GB happens at 30% dimensionless volume. The ratio of the work done on the viscous pressure response to the elastic energy was defined and worked out, the stiffness of the elastic pressure-volume curve was extracted. It was indicated that the GB stimulated with CCK or treated with indomethacin is subject to almost constant stiffness at low volume ($\leq$ 70% dimensionless volume) but rapidly increasing stiffness at high volume ($>$ 70% dimensionless volume) and a larger work-to-energy ratio (0.57-0.61) compared with the normal GB in passive state. Th models are sensitive to the change in the biomechanical property when a GB was stimulated with CCK or treated with indomethacin, showing a potential in clinical application. Further work should be devoted to applying these methods to intact GB pressure-volume curves at various frequencies of infusion-withdrawal cycle so as to establish effects of the frequency on the elastic and viscous responses.

Reference

[1] Cotton P B, Elta G H and Carter C R, et al, Gallbladder and sphincter of Oddi disorders, Gastroenterology, 2016, 150(6), 1420-1429

[2] Wald A, Functional biliary-type pain, Journal of Clinical Gastroenterology, 2005, 39(S3), S217-S222

[3] Misra D C, Blosssom G B, Fink-Bennett D, et al, Results of surgical therapy for biliary dyskinesia, Archive of Surgery, 1991,126(8), 957-960

[4] Yap L, Wycherly A G, Morphett A D, et al, Acalculous biliary pain: cholecystectomy alleviates symptoms in patients with abnormal cholescintigraphy, Gastroenterology, 1991,101(3), 786-793

[5] Halverson J D, Garner B A, Siegel B A, et al, The use of hepatobiliary scintigraphy in patients with acalculous biliary colic, Achieve Internal Medicine, 1992, 152(6), 1305-107

[6] Kloiber R, Molnar C P and Shaffer E A, Chronic biliary-type pain in the absence of gallstones: the values of cholecystokinin cholescintigraphy, American Journal of Roentgenology, 1992, 159(3), 509-513

[7] Sorenson M K, Fancher S and Lang N P, et al, Abnormal gallbladder nuclear ejection fraction prediction success of cholecystectomy in patients with biliary dyskinesia, American Journal of Surgery, 1993, 166(6), 672-675

[8] Smythe A, Majeed A, Fitzhebry M et al, A requiem for the cholecystokinin provocation test?, Gut, 1998, 43(4), 571-574

[9] Canfield A J, Hetz S P, Schriver J P, et al, Biliary dyskinesia: a study of more than 2000 patients and review of the literature, Journal of Gastrointestinal Surgery, 1998, 2(5), 443-448

[10] Yost F, Margenthalaer J, Presti M, et al, Cholecystokinin is an effective treatment for biliary dyskinesia, American Journal of Surgery, 1999, 178(6), 462-465

[11] Merg A R, Kalinowski S E, Hinkhous M M, et al, Mechanisms of impaired gallbladder contractile response in chronic acalculous cholecystitis, Journal of Gastrointestinal Surgery, 2002, 6(3), 432-437

[12] Lim J U, Joo K R, Won K Y, et al, Predictor of abnormal gallbladder ejection fraction in patients with atypical biliary pain: Histopathological point of view, Medicine (Baltimore), 2017, 96(51), e9269

[13] Li W G, Luo X Y, Hill N A, et al, Correlation of mechanical factors and gallbladder pain, Computational & Mathematical Methods in Medicine, 2008, 9(1), 27-45

[14] Li W G, Luo X Y, Hill N A, et al, A mechanical model for CCK-induced acalculous gallstone pain, Annals of Biomedical Engineering, 2011, 39(2), 786-800

[15] Schoetz D J, Lamore W W, Wise W E, et al, Mechanical properties of primate gallbladder description by a dynamic method, American Journal of Physiology-Gastrointestinal Liver Physiology, 1981, 41, G376-G381.

[16] Brotschi E A, Lamore W W and Williams L F, Effect of dietary cholesterol and indomethacin on cholelithiasis and gallbladder motility in guinea pig, Digestive Diseases and Sciences, 1984, 29(11), 1050--1056

[17] Kaplan G S, Bhutani V K, Shaffer T H, et al, Gallbladder mechanics in newborn piglets, Pediatric Research, 1984, 18(11), 1181-1184

[18] Matsuki Y, Dynamic stiffness of the isolated guinea pig gall-bladder during contraction induced by cholecystokinin, Japanese Journal of Smooth Muscle Research, 1985, 21(6), 427-438

[19] Goto M and Kimoto Y, Hysteresis and stress-relaxation of the blood vessels studied by a universal tensile testing instrument, Japanese Journal of Physiology, 1966, 16(2), 169-184

[20] Gow B S and Taylor M G, Measurement of viscoelastic properties of arteries in the living dog, Circulation Research, 1968, 23(1), 111-122

[21] Azuma T and Hasegawa M, A rheological approach to the architecture of arterial walls, Japanese Journal of Physiology, 1971, 21(1), 27-47

[22] Gow B S, Schonfeld D and Patel D, The dynamics elastic properties of the canine left circumflex coronary artery, Journal of Biomechanics, 1974, 7(5), 389-395

[23] Cox R H, Viscoelastic properties of canine pulmonary arteries, American Journal of Physiology-Heart and Circulatory Physiology, 1984, 246, H90-H96

[24] Remington J W and Alexander R S, Stretch of the bladder as an approach to vascular distensibility, American Journal of Physiology, 1955, 181(2), 240-248,

[25] Rankin J S, Arentzen C E, McHale P A, et al, Viscoelastic properties of the diastolic left ventricle in the conscious dog, Circulation Research, 1977, 41(1), 37-45

[26] Starc V, Yellin E L and Nikolic S D, viscoelastic behavior of the isolated guinea pig left ventricle in diastole, American Journal of Physiology-Heart and Circulatory Physiology, 1996, 271, H1314-H1324

[27] van Duyl W A, A model for both the passive and active properties of urinary bladder tissue related to bladder function, Neurourology and Urodynamics, 1985, 4(4), 275-283

[28] Kondo A and Susset J G, Physical properties of the urinary detrusor muscle, Journal of Biomechanics, 1973, 6(2), 141-151

[29] Glantz S A, A constitutive equation for the passive properties of muscle, Journal of Biomechanics, 1974, 7(2), 137-145

[30] Sanjeevi R, A viscoelastic model for the mechanical properties of biological materials, Journal of Biomechanics, 1982, 15(2), 107-109

[31] Vandenbrouck A, Laurent H, Hocine N A, et al, A hyperelasto-visco-hysteresis model for an elastomeric behaviour: Experimental and numerical investigations, Computational Materials Science, 2010, 48, 495-503

[32] Panda S K and Buist M L, A viscoelastic framework for inflation testing of gastrointestinal tissue, Journal of Mechanical Behavior of Biomedical Materials, 2020, 103, 103569

[33] Westerhof N and Noordergraaf A, Arterial viscoelasticity: a generalized model, Journal of Biomechanics, 1970, 3(3), 357-379

[34] Cox R H, A model for the dynamic mechanical properties of arteries, Journal of Biomechanics, 1972, 5(2), 135-152

[35] Goedhard W J A and Knoop A A, A model of the arterial wall, Journal of Biomechanics, 1973, 6(3), 281-288

[36] Woo S L Y, Gomez M A and Akeson W H, The time and history-dependent viscoelastic properties of the canine medical collateral ligament, ASME Journal of Biomechanical Engineering, 1981, 103(4), 293-297

[37] Provenzano P, Lakes R, keenan T, et al, Nonlinear ligament viscoelasticity, Annals of Biomedical Engineering, 2001, 29(10), 908–914

[38] Goh S M, Charalambides M N and Williams J G, Determination of the constitutive constants of non-linear viscoelastic materials, Mechanics of Time-Dependent Materials, 2004, 8, 255-268

[39] Abramowitch S D, Woo S L Y, Clineff T D, et al, An evaluation of the quasi-linear viscoelastic properties of the healing medial collateral ligament in a goat model, Annals of Biomedical Engineering, 2004, 32(3), 329–335

[40] Pena E, Calvo B, Martinez M A, et al, An anisotropic visco-hyperelastic model for ligaments at finite strains: formulation and computational aspects, International Journal of Solids and Structures, 2007, 44(3-4),760–778

[41] Lim Y J, Deo D and Singh T P, et al, In situ measurement and modelling of biomechanical response of human cadaveric soft tissues for physics-based surgical simulation, Surgical Endoscopy, 2009, 23, 1298-1307

[42] Pena J A, Martinez M A and Pena E, A formulation to model the nonlinear viscoelastic properties of the vascular tissue, Acta Mechanica, 2011, 217(1), 63–74

[43] Yang T, Chui C K, Yu R Q, et al, Quasi-linear viscoelastic modelling of arterial wall for surgical simulation, International Journal of Computer Assisted Radiology and Surgery, 2011, 6(6), 829-838

[44] Natali A N, Pavan P G, Venturato C, et al, Constitutive modeling of the non-linear visco-elasticity of the periodontal ligament, Computer Methods and Programs in Biomedicine, 2011, 104(2), 193–198

[45] Davis F M and De Vita R, A nonlinear constitutive model for stress relaxation in ligaments and tendons, Annals of Biomedical Engineering, 2012, 40(12), 2541-2550

[46] Davis F M and De Vita R, A three-dimensional constitutive model for the stress relaxation of articular ligaments, Biomechanics and Modeling in Mechanobiology, 2014, 13(3),653–663

[47] Babaei B, Abramowitch S D and Elson E L, et al, A discrete spectral analysis for determining quasi-linear viscoelastic properties of biological materials, Royal Society Interface, 2015, 12, 2050707, http://dx.doi.org/10.1098/rsif.2015.0707

[48] Criscenti G, De Maria C, Sebastiani E, et al, Quasi-linear viscoelastic properties of the human medial patello-femoral ligament, Journal of Biomechanics, 2015, 48(16), 4297-4302

[49] Ghahfarokhi Z M, Zand M M, Tehrani M S, et al, A visco-hyperelastic constitutive model of short- and long-term viscous effects on isotropic soft tissues, Proc IMechE Part C: Journal Mechanical Engineering Science, 2020, 234(1) 3–17

[50] Pioletti D P, Rakotomanana L R, Benvenuti J F, et al, Viscoelastic constitutive law in large deformations: application to human knee ligaments and tendons, Journal of Biomechanics, 1998, 31(8), 753-757

[51] Pioletti D P and Rakotomanana L R, Non-linear viscoelastic laws for soft biological tissues, European Journal of Mechanics-A/Solids, 2000, 19 (5), 749-759

[52] Lu Y T, Zhu H X, Richmond S, A visco-hyperelastic model for skeletal muscle tissue under high strain rates, Journal of Biomechanics, 2010, 43(13), 2629–2632

[53] Ahsanizadeh S and Li L P, Visco-hyperelastic constitutive modeling of soft tissues based on short and long-term internal variables, BioMedical Engineering OnLine, 2015, 14(29), doi 10.1186/s12938-015-0023-7 (16 pages)

[54] Limbert G and Middleton J, A transversely isotropic viscohyperelastic material Application to the modeling of biological soft connective tissues, International Journal of Solids and Structures, 2004, 41(15), 4237-4260

[55] Kulkarni S G, Gao X L, Horner S E, et al, A transversely isotropic visco-hyperelastic constitutive model for soft tissues, Mathematics and Mechanics of Solids, 2016, 21(6), 747–770

[56] Vogel A, Rakotomanana L and Pioletti D P, Chapter 3-viscohyperelastic strain energy function, In: Biomechanics of Living Organs-Part 1, Edited by Payan Y and Ohayon J, London: Academic Press, 2017, https://doi.org/10.1016/B978-0-12-804009-6.00003-1, 59-78

[57] Yousefi A K, Nazari M A, Perrier P, et al, A visco-hyperelastic constitutive model and its application in bovine tongue tissue, Journal of Biomechanics, 2018, 71, 190-198

[58] Yamada K, Matsumura Y, Suzuki H, et al, The histochemistry of collagens and fibronectin in the gallbladders of the guinea pig and mouse, Acta Histochemica et Cytochemica, 1989, 22(6), 675-683

[59] Li W G, Luo X Y, Hill N A, et al, Cross-bridge apparent rate constants of human gallbladder smooth muscle, Journal of Muscle Research and Cell Motility, 2011, 32, 209–220

[60] Gestrelius S and Borgstron P, A dynamic model of smooth muscle contraction, Biophysical Journal, 1986, 50(1), 157-169

[61] Schmitz A and Bol M, On a phenomenological model for active smooth muscle contraction, Journal of Biomechanics, 2011, 44, 2090-2095

[62] Bauer R D, Busse R, Schabert A, et al, Separate determination of the pulsatile elastic and viscous developed in the arterial wall in vivo, European Journal of Physiology, 1979, 380(3), 221-226

[63] Pomeranz I S and Shaffer E A, Abnormal gallbladder emptying in a subgroup of patients with gallstones, Gastroenterology, 1985, 88(3), 787-91

[64] Yau W M, Makhouf G M, Edwards L E, et al, Mode of actin of cholecystokinin and related peptides on gallbladder muscle, Gastroenterology, 1973, 65, 451-456

[65] Krishnamurthy S and Krisbnamurthy G T, Biliary dyskinesia: Role of the sphincter of oddi, gallbladder and cholecystokinin, Journal of Nuclear Medicine, 1997, 38(11), 1824-1830

[66] Doggrell S A and Scott G W, The effect of time and indomethacin on contractile response of the guinea-pig gall bladder in vitro, British Journal of Pharmacology, 1980, 71(2), 429-434

[67] Kotwall C A, Clanachan A S, Baer H P, et al, Effects of prostaglandins on motility of gallbladders removed patients with gallstones, Archive of surgery, 1984, 119(6), 709-712

[68] O'Donnell L J D, Wilson P, Guest P, et al, Indomethacin and postprandial gallbladder emptying, Lancet, 1992, 339(8788), 269-271

[69] Parkman H P, James A N, Thomas R M, et al, Effect of indomethacin on gallbladder inflammation and contractility during acute cholecystitis, Journal of Surgical Research, 2001, 96(1), 135-142

[70] Murray F E, Stinchcombe S J and Hawkey C J, Effect of indomethacin and misoprostol on fast gallbladder volume and meal-induced gallbladder contractility in humans, Digestive Diseases and Sciences 1992, 37(8), 1228-1231

[71] Li W G, Hill N A and Ogden R W, et al, Anisotropic behaviour of human gallbladder walls, Journal of Mechanical Behavior of Biomedical Materials, 2013, 20, 363-375

[72] Ryan J and Cohen S, Gallbladder pressure-volume response to gastrointestinal hormones, American Journal of Physiology, 1976, 230(6), 1461-1465

[73] Miura K and Saito S, Visco-elastic properties of the gallbladder in rabbit and guinea-pig, Journal of Showa Medical Association, 1967, 27(2), 135-138

[74] Borly L, Hojgaard L, Gronvall S, et al, Human gallbladder pressure and volume: validation of a new direct method for measurements of gallbladder pressure in patients with acute cholecystitis, Clinical Physiology, 1996, 16(2), 145-156

Appendix A Validation of Proposed GB Pressure-Volume Model

Traditionally, experimental GB pressure-volume curves are considered as a parabola of volume either in passive state or in active state [72]. However, this mathematical model does not seem to be general. A more general mathematical model is put forward by Eq. (13), which is written as the following in terms of GB volume

$$p_e = p_{e,exp}(0) + c_0 V + c_1 V^{n_1} + c_2 e^{c_3 V^{n_2}} \tag{19}$$

where $p_{e,exp}(0)$ is the GB pressure at V=0 in an experiment, the model constants c_0, c_1, c_2, c_3, n_1 and n_2 will be optimized based on the experimental data in [72-74]. The first three terms in Eq. (19) represent the GB response to a small variation in volume, while the last term is the response to a large change in volume.

The experimental data and Eq.(19) are programmed in MATLAB® R2018b by employing its *lsqnonlin* function in terms of trust-region-reflective optimization algorithm. The accuracy of the optimization is assessed by the error ε_p defined as

$$\varepsilon_p = \frac{\sqrt{\sum_{i=1}^{N}[p_e(V_i) - p_{e,exp}(V_i)]^2}}{\sum_{i=1}^{N} p_{e,exp}(V_i)} \times 100\% \tag{20}$$

where $p_{e,exp}(V_i)$ and $p_e(V_i)$ are the experimental GB pressure and the pressure predicted with Eq.(20) at an experimental point i, N is the number of total experimental points in a GB pressure-volume test.

The five model constants optimized, and the corresponding errors based on the experimental data in [72-74] are listed in Table 2. The comparison between measurements and predictions is demonstrated in Fig.9. It is shown that these errors are less than 4%, and the excellent agreement has been achieved between them. Thus, the mathematical model works well in fitting a variety of GB pressure-volume curves in passive and active states.

Table 1 Model constants optimized in pressure decomposition and pressure-volume curve fitting in passive and active states

GB state	Viscous property		Elastic property		
	Constant & error	Value	Constant	Value	ε_p(%)
Passive	a_1	4.3667×10^{-1}	c_0	10.2740	0.41
	a_2	-8.9372×10^{-3}	c_1	9.0932	
	a_3	4.5843×10^{-5}	n_1	4.2455	
	m_1	1.2801	c_2	3.0288×10^{-7}	
	ε_1(%)	1.63	c_3	15.2020	
			n_2	9.9131	
Active	b_1	6.3195×10^{1}	c_0	1.1972×10^{1}	0.69
	b_2	-1.0000×10^{2}	c_1	4.4048	
	b_3	3.8962×10^{1}	n_1	4.9091×10^{-10}	
	m_2	3.5578×10^{-2}	c_2	1.2123×10^{-1}	
	ε_2(%)	1.61	c_3	4.1278	
			n_2	2.7313	
Indomethacin	a_1	8.4342×10^{-1}	c_0	4.8221	0.40
	a_2	-8.3111×10^{-2}	c_1	1.4452	
	a_3	2.1309×10^{-3}	n_1	4.8451×10^{-1}	
	m_1	1.1403	c_2	2.9176×10^{-3}	
	ε_1(%)	1.16	c_3	7.4109	
			n_2	1.0950	

Table 2 Model constant in curve fitting of experimental GB pressure-volumes for rabbit, opossum, guinea-pig and human

Subject	GB state	c_0	c_1	n_1	c_2	c_3	n_2	ε_V(%)
Rabbit	Passive	$3.6042\times10^{2-7}$	2.0129×10^{2}	1.3056	2.2217×10^{-12}	6.9320×10^{-2}	2.2690×10^{3}	0.77
Guinea-pig	Passive	2.0604×10^{-11}	1.8016×10^{2}	1.9912	4.1973×10^{-3}	7.5274	1.2983×10^{-3}	0.93
Opossum	Passive	4.3027	8.3306	3.8686	7.4789×10^{-8}	1.8417×10^{1}	7.5515×10^{-2}	0.51
	CCK1	2.2204×10^{-12}	2.5366×10^{1}	1.7892	2.2927×10^{-12}	2.5131×10^{-11}	9.8952	0.85
	CCK2	2.5080×10^{-12}	3.1371×10^{1}	1.5439	1.3661×10^{-3}	7.1110	2.2018×10^{-7}	1.60
	CCK3	8.1729×10^{-1}	1.5132×10^{1}	1.2999	6.7502×10^{-8}	19.1570	1.7679×10^{-1}	1.42
Patient	8,passive	0.0000	4.7436×10^{2}	1.3425	9.6891×10^{-4}	6.6498	2.2884×10^{-9}	3.85
	9,passive	0.0000	6.2864	0.2599	6.1851×10^{-6}	1.4637×10^{1}	3.4060×10^{-1}	1.36
	10,passive	5.8161	1.7439×10^{1}	2.6326	4.7908×10^{-9}	2.2059×10^{1}	5.6654×10^{-1}	2.08
	11,passive	1.1618×10^{1}	3.8518×10^{1}	7.0642	2.5796×10^{-1}	1.9855×10^{-2}	6.9929	1.78

CCK1=0.025μg/kg.h, CCK2=0.25μg/kg.h, CCK3=2.5μg/kg.h

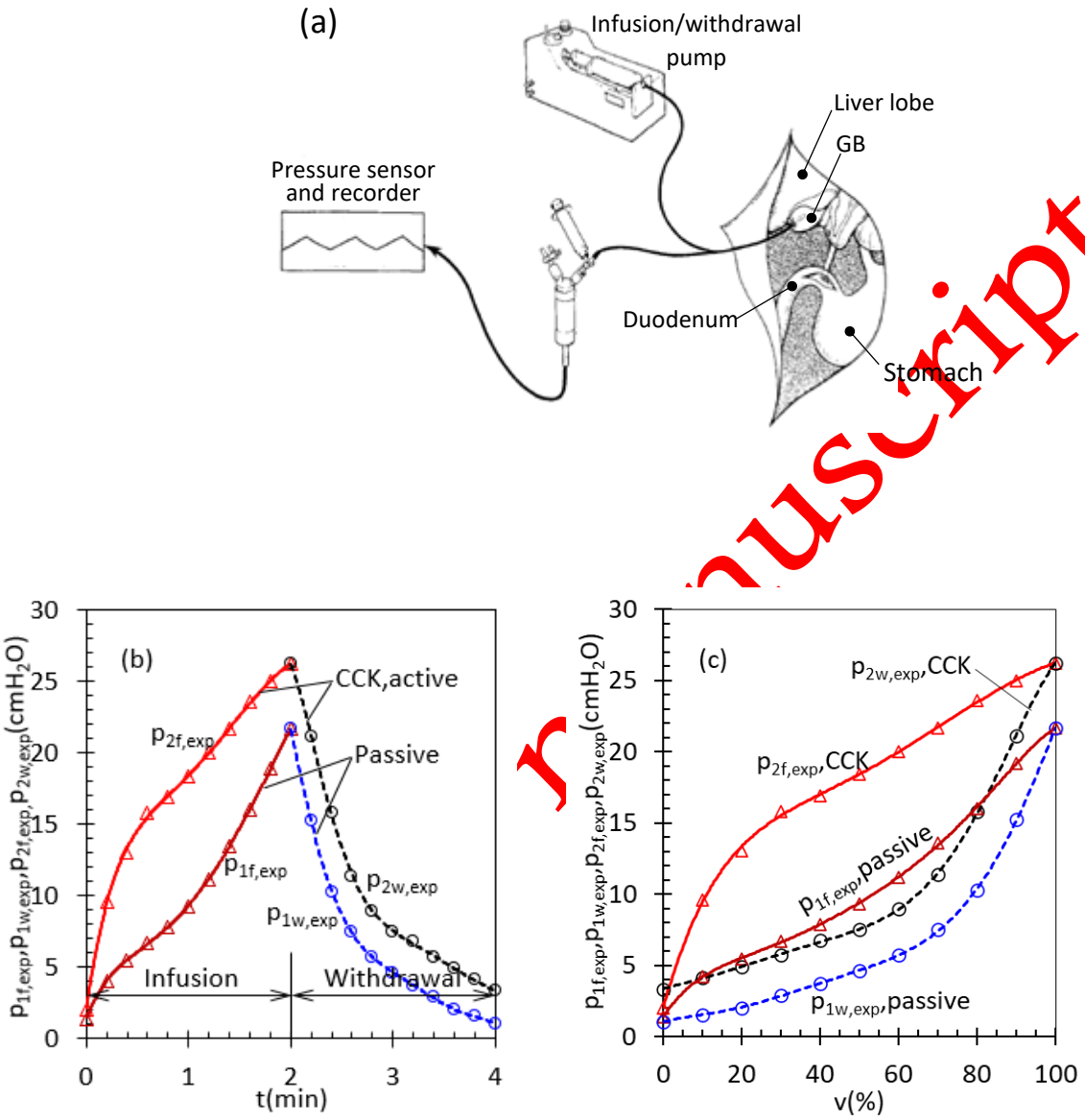

Fig.1 The sketch of experimental preparation of a guinea pig for GB pressure-volume measurements in vitro (a), pressure-time history curve (b) and pressure-volume curve (c) under passive and CCK stimulated conditions for the same GB in [16], the GB volume is expressed with percentage of the maximum GB volume, (a) is adapted from [16]

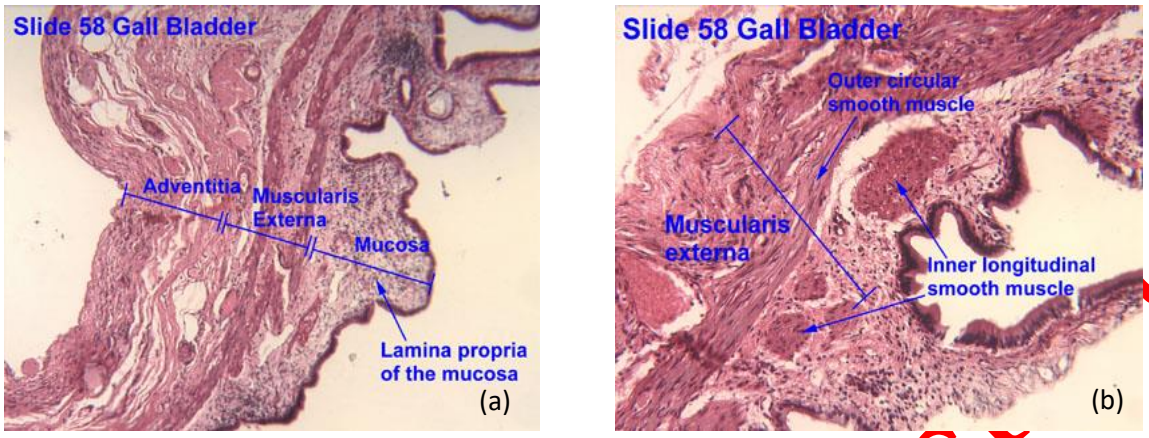

Fig.2 The GB wall histology, (a) three-layer structure in longitudinal cross-selection, (b) muscle layer in circumferential cross-section, these pictures are from https://www.ouhsc.edu/histology/Glass%20slides/58_05.jpg, https://www.ouhsc.edu/histology/Glass%20slides/58_08.jpg

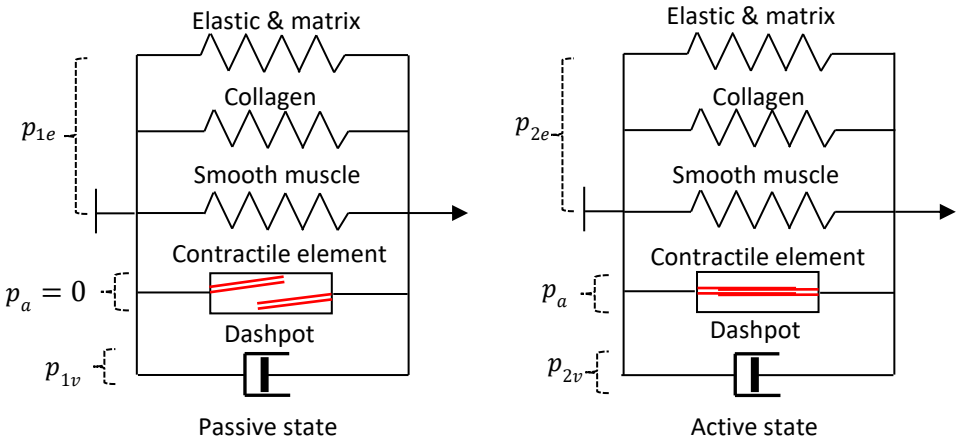

Fig.3 The proposed biomechanical viscoelastic discrete model in time domain for the pressure-volume curve of GBs in passive and active states, p_a=0 in passive state

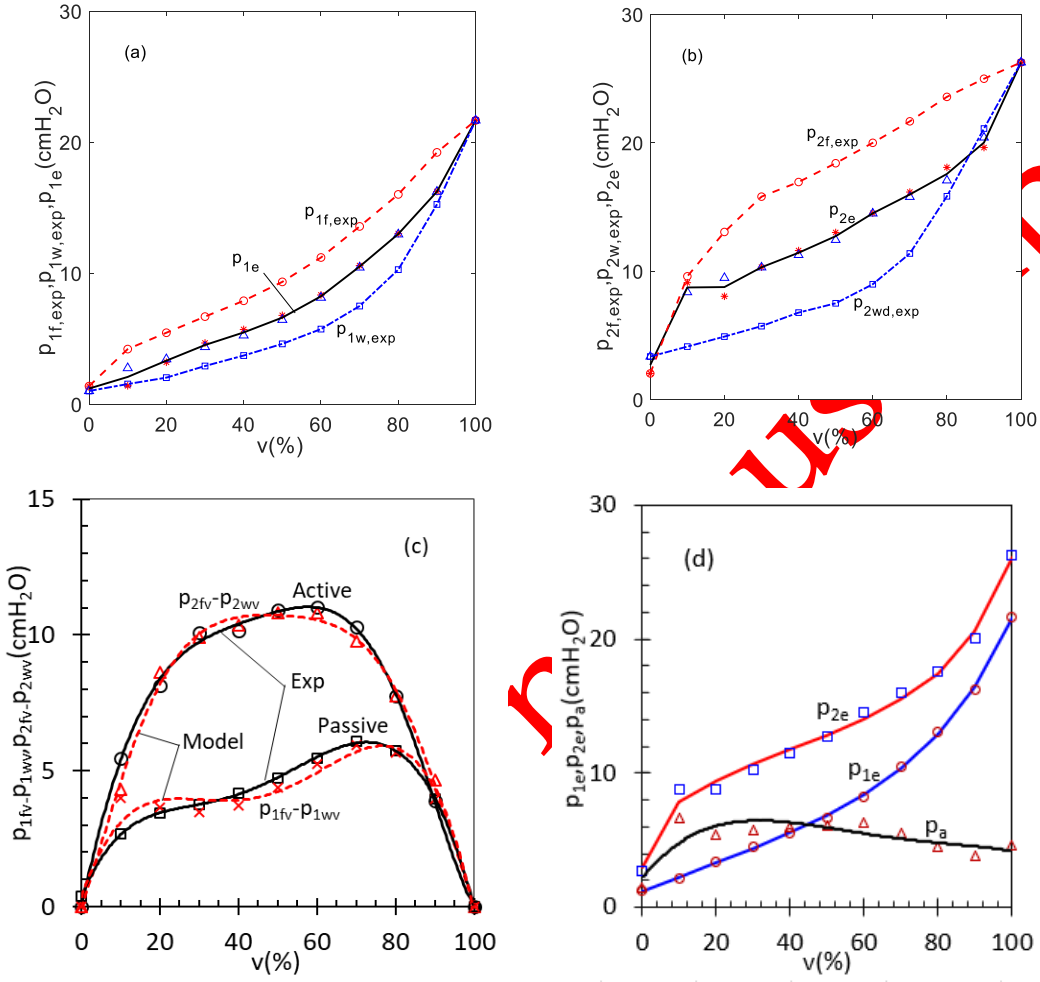

Fig.4 The discomposed pressure responses to dimensionless volume change in a guinea-pig GB in both passive and active states, (a) passive, (b) active, (c) viscous, (d) elastic passive pressure and active pressure, the symbols are for experimental data, the lines in (a) and (b) are not fitting curves

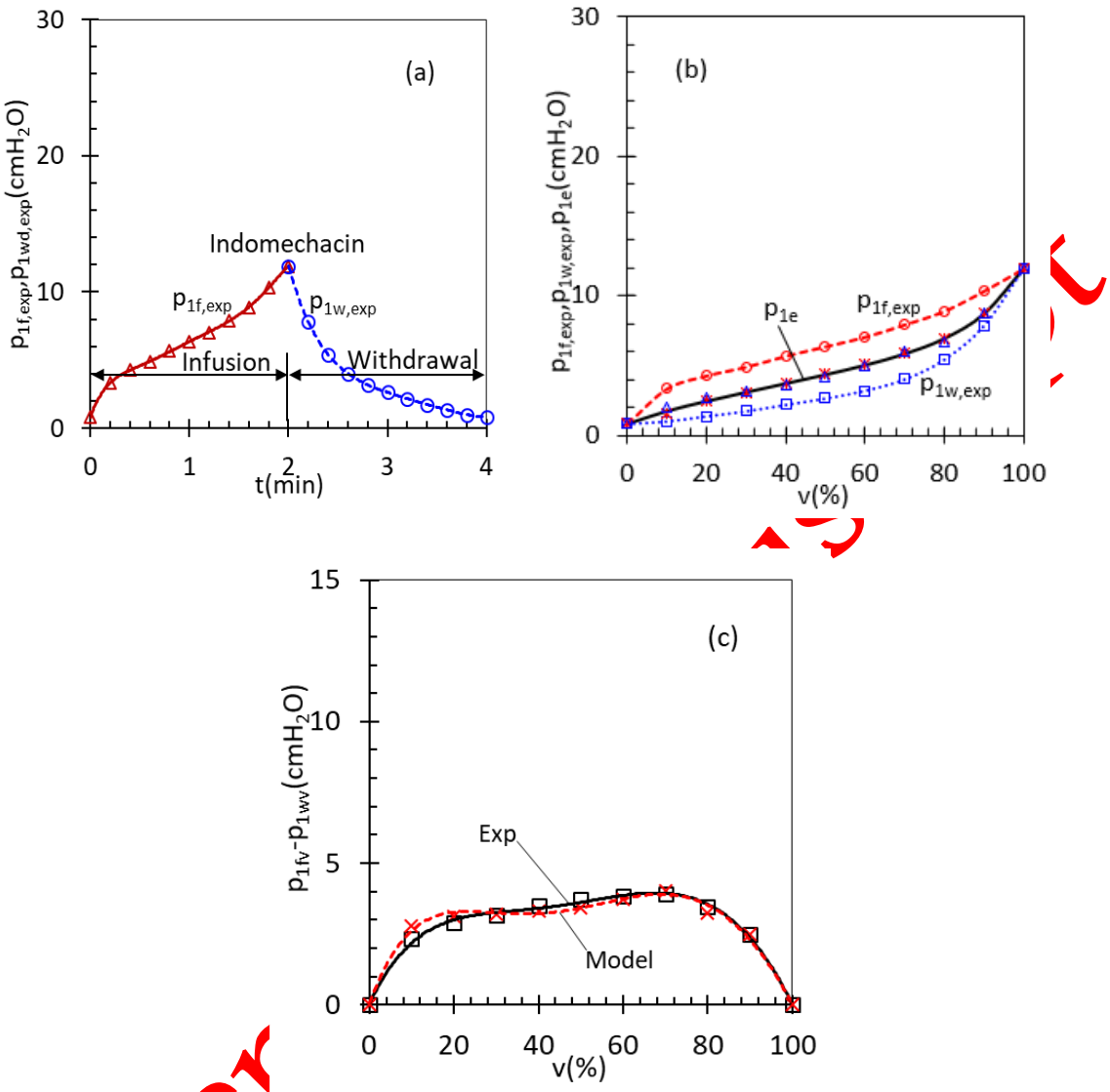

Fig.5 The experimental pressure-time curves (a), pressure-volume-time curves and discomposed pressure responses (b), viscous pressure response (c) to dimensionless volume change in a guinea-pig GB in passive state treated with indomethacin, the scattered points are for experimental data, the curves for model predictions

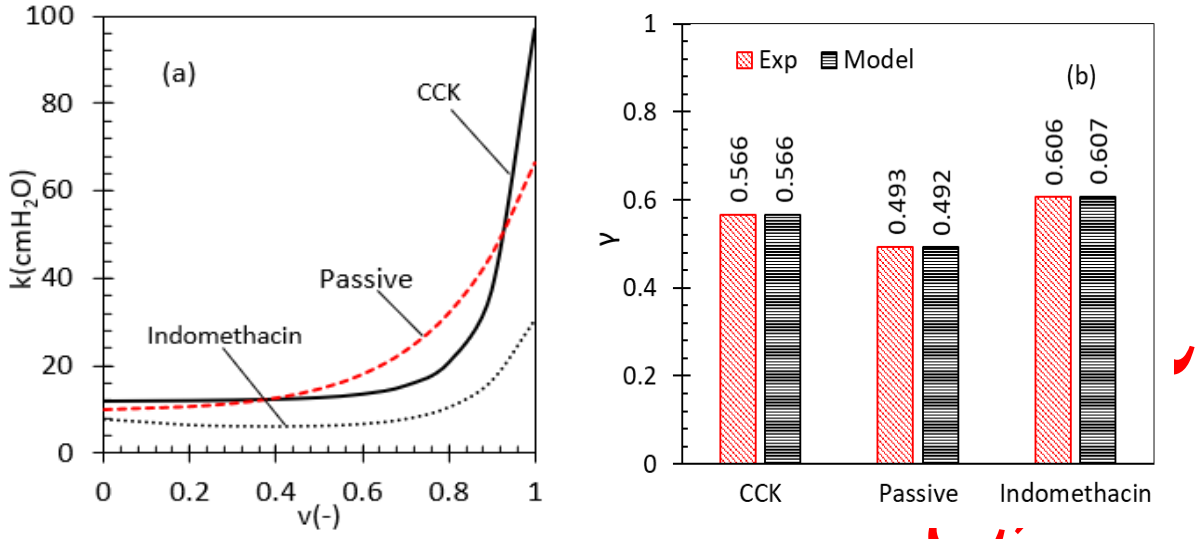

Fig.6 The elastic stiffness k (a) and the ratio of the work done on the viscous response to the elastic energy stored in GB wall γ (b) in active state stimulated with CCK, passive state in control, and passive state treated with indomethacin

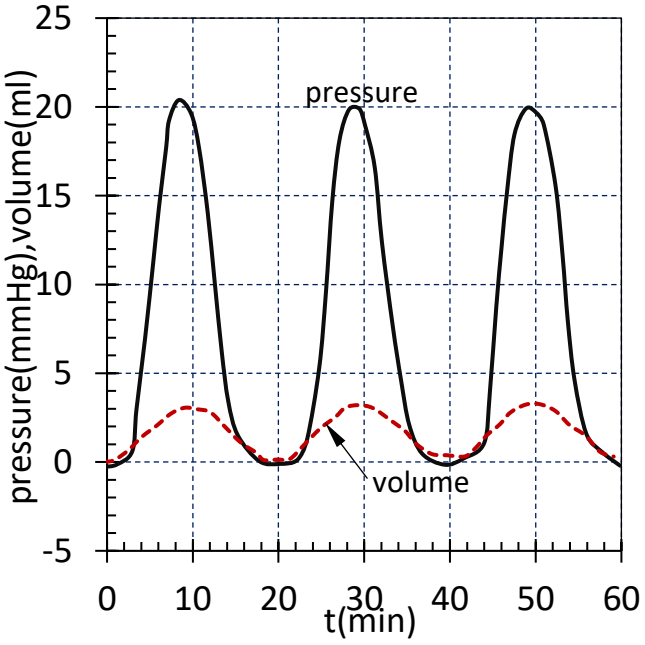

Fig.7 The typical pressure-time and volume-time curves of a baboon intact GB in passive state measured in [15]

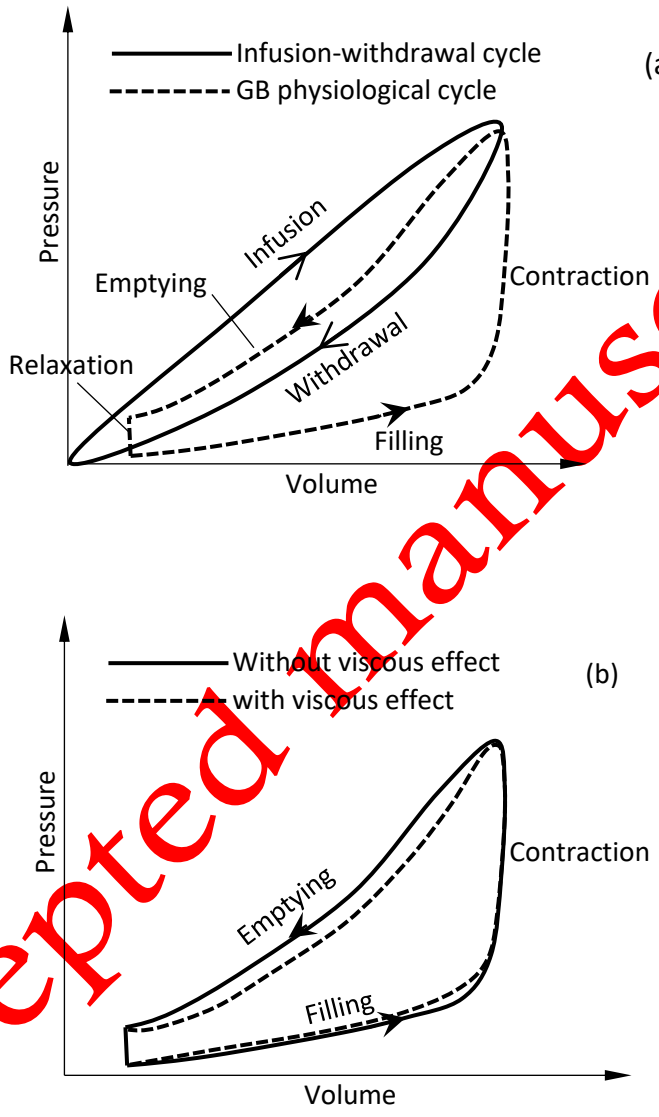

Fig.8 The comparison of in vitro infusion-withdrawal cycle experiment and GB emptying-filing physiological cycle, (a) comparison of two cycles, (b) effect of GB wall viscosity on GB emptying-filling cycle

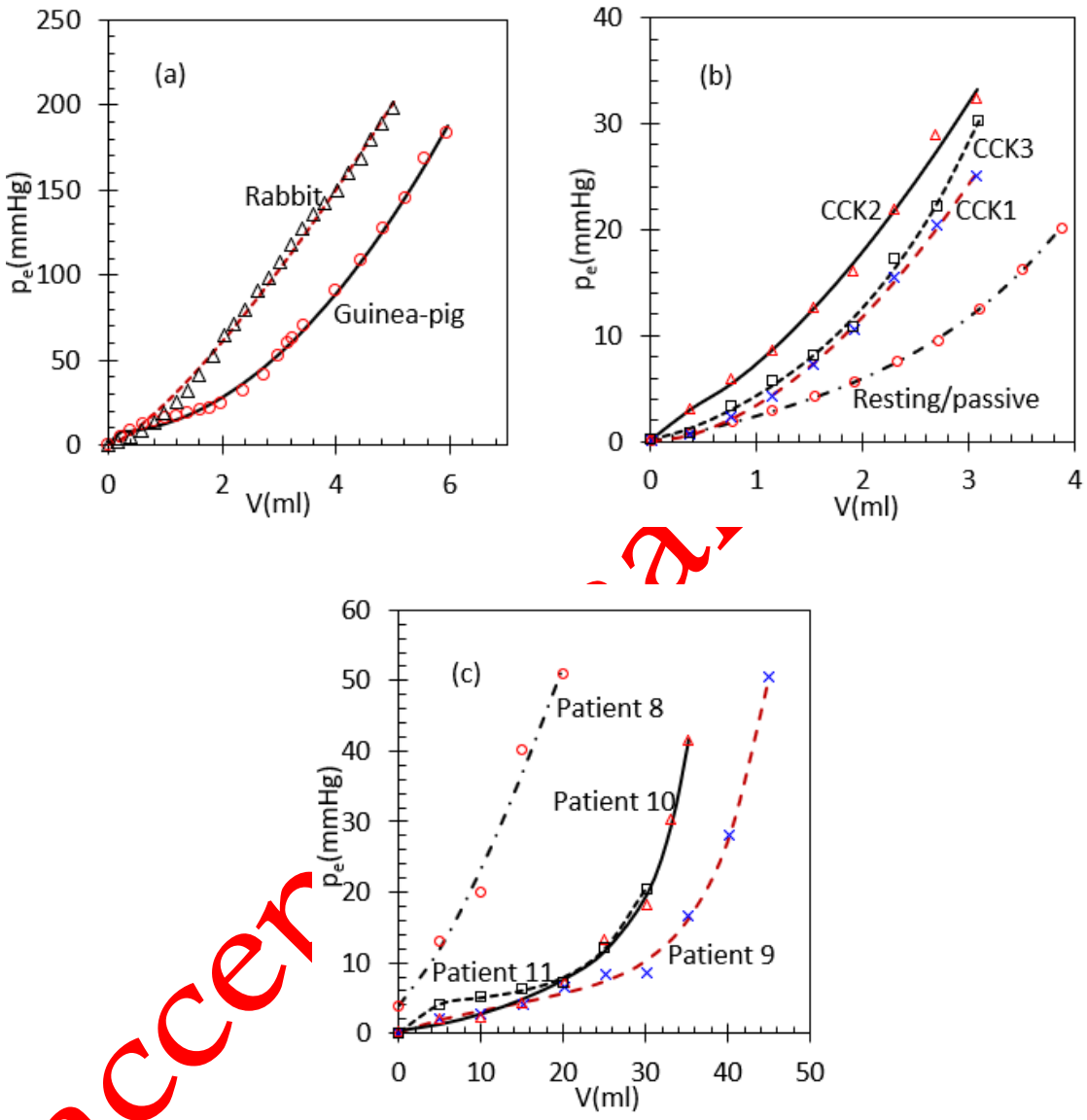

Fig.9 The comparison of GB pressure-volume curves predicted by using the mathematical model with the experimental data, (a) pressure-volume curves of rabbit and guinea-pig in passive state [73], (b) pressure-volume curves of opossum in passive and active states [72], (c) pressure-volume curves of patients with acute cholecystitis in passive state [74]